I&EC research
Industrial & Engineering Chemistry Research

Article

pubs.acs.org/IECR

Ethanol Steam Reforming Thermally Coupled with Fuel Combustion in a Parallel Plate Reactor

Eduardo Lopez,[†,‡,*] Vanessa Gepert,[†,§] Achim Gritsch,[†,∥] Ulrich Nieken,[†] and Gerhart Eigenberger[†]

[†]Institute for Chemical Process Engineering (ICVT), University of Stuttgart, Böblinger Strasse 72/78, 70199 Stuttgart, Germany

[‡]Planta Piloto de Ingeniería Química (PLAPIQUI), National Research Council of Argentina, Camino La Carrindanga km. 7, 8000 Bahía Blanca, Argentina

ABSTRACT: This contribution reports experimental studies of ethanol steam reforming for the production of a hydrogen-rich reformate for fuel cells. A Pd-based catalyst, coated on corrugated metallic structures, was used. Axial concentration profiles for all components present in the system were measured in a kinetic reactor under isothermal conditions for different temperatures, flow rates, and steam-to-carbon ratios. Appropriate activity and hydrogen selectivity were achieved for this catalytic system at 650 °C, with complete ethanol conversion (no acetaldehyde), ca. 5% carbon monoxide and 1% methane as byproducts. For reactor modeling in an appropriate range of operating conditions, a simple global kinetics model is proposed; the correspondent parameters were fitted to the experimental data. Thermal coupling between ethanol steam reforming and hydrogen combustion was experimentally studied for subsequent implementation in a parallel-plate reactor, preferably in a so-called folded plate reactor. A single unit of this reactor, consisting of one combustion channel in between two halves of reforming channels was selected for the experimental proof-of-concept. The influence of different operating variables (ethanol load, feed distribution of the combustion fuel along the channel length, operation temperature, and steam-to-carbon ratio) on the reactor performance and the thermal coupling pattern will be discussed.

1. INTRODUCTION

Electrical power generation by fuel cells becomes increasingly attractive for stationary and mobile applications because of its improved conversion efficiency and environmental impact. Among the different types of fuel cells, the proton exchange membrane (PEM) fuel cell appears to be the most promising for application in vehicles or small scale decentralized power stations. The required hydrogen fuel can be generated in situ by steam reforming of hydrocarbons or alcohols. The use of bioethanol (of nonfossil origin) as feedstock is of particular interest since it results in an almost closed CO_2 generation loop.[1−3] In addition, a diluted ethanol/water mixture can be used as feed, which strongly reduces energy consumption for distillative ethanol concentration.

In traditional reactor concepts, the strongly endothermic steam reforming reaction is subject to severe heat transfer limitations between the reforming catalyst and the heat source. Heat integrated wall reactor concepts, where both the reforming and the combustion catalyst are deposited at opposite sides of the heat transferring walls, allow for a substantial reduction of the heat transfer resistance. The potential of wall reactors to control the operating conditions of steam reforming reactions has been demonstrated elsewhere.[4−13] Several examples of the exploitation of the wall reactor concepts in microreactors for hydrogen production are reported by Kolb and Hessel[14] and Kiwi-Minsker and Renken.[15]

Among heat integrated wall reactors, the folded-plate reactor (FPR) concept[16,17] presents an interesting option (Figure 1). In this design, a folded metal sheet divides the reactor volume into two chambers with narrow channels in the range of 1 to 5 mm width. Each chamber is open to one side, allowing distributing side feeds along the entire length of the channels. This proved to be of substantial advantage for the direct coupling of exo- and endothermic reactions.[8,9] Corrugated spacers in the channels act as fins for improving the heat exchange, as static mixers and as catalyst supports. On each side, the reactor properties can be structured axially through the selection of catalyst-coated or uncoated spacers. Lab- and pilot-scale FPR-prototypes have been successfully designed and operated at the Institute for Chemical Process Engineering (ICVT), University of Stuttgart, as catalytically heated evaporators, liquid-cooled (isothermal) reactors, heat-exchanger reactors for waste-gas purification and co- and countercurrent reactors for coupling steam reforming of methanol or methane with auxiliary combustion reactions.[5,7−9,18−24]

The present contribution proposes an FPR for decentralized ethanol steam reforming for hydrogen production. In every second channel of the reactor, the endothermic steam reforming reaction is performed, while the necessary heat of reaction is provided by hydrogen combustion in the alternate channels.

Corrugated spacers, washcoated with Pd-based catalyst were used in both channel types to conduct the ethanol reforming and the hydrogen combustion. Reaction kinetics for the ethanol steam reforming in the range of practical interest have been determined under well-defined isothermal conditions in an integral reactor and are represented by mass action type rate equations.

Received: February 28, 2011
Revised: February 20, 2012
Accepted: February 28, 2012
Published: February 28, 2012

dx.doi.org/10.1021/ie202364y | *Ind. Eng. Chem. Res.* 2012, 51, 4143−4151

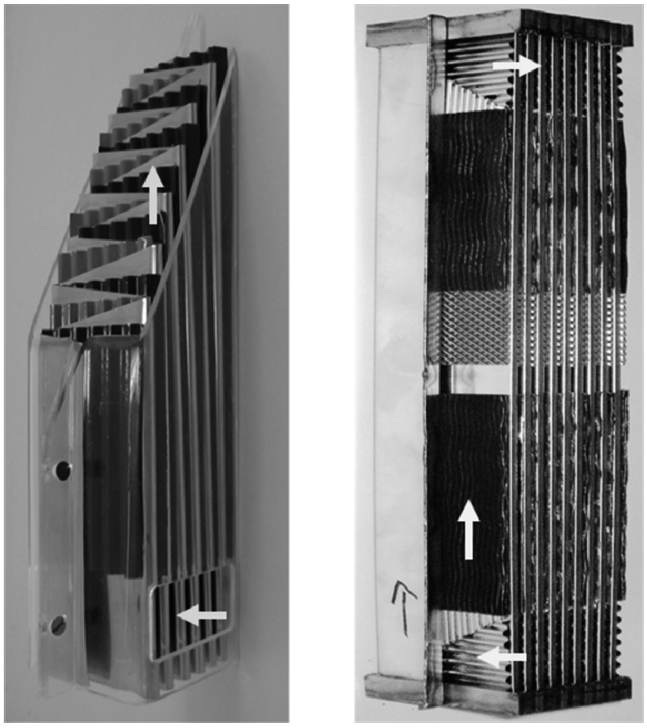

Figure 1. Model of a folded plate reactor (left) and interior of a folded plate reactor prototype for methane steam reforming.[9,27]

To experimentally test the thermal coupling of ethanol steam reforming with hydrogen combustion, a so-called "sandwich reactor" (SR) was used.[6,9] It is considered to represent a two channel section of the final multichannel reactor and comprises of one combustion channel, sandwiched between two reforming channels. Experimental results for different operating conditions and different side feed configurations for the combustion channel will be presented.

2. REACTION KINETICS

2.1. Kinetic Reactor. An isothermal flat-bed reactor was selected to test the performance of the Pd/γAl_2O_3-coated catalytic spacers for ethanol steam reforming (Engelhard, commercial oxidation catalyst). As shown in Figure 2a, the catalyst-coated spacer, forming 40 parallel channels of 0.94 mm hydraulic diameter, is placed in a stainless steel casing (40 mm width, 1.2 mm height). Three catalyst sections, each of 50 mm length, with an external catalyst surface of about 64 cm^2 each, have been used in sequence. Between the sections void spaces allow to withdraw gas samples over side ports for composition analysis and temperature measurement, as shown in Figure 2b. High temperature resistant stainless steel 1.4835 was used for both the spacers and the reactor casing. During kinetic measurements, this material showed no signs of carburization or metal dusting. The flat-bed reactor is thermostatted by heating cartridges which are placed in metal blocks H1 to H10 on both sides of the casing. This design provides well-controlled temperature conditions along the length of the flat bed reactor. Uniform entrance flow conditions are achieved by mixing elements in the inlet region. The kinetic reactor is connected to an appropriate periphery, consisting of water and ethanol evaporators, reactant feeds through mass-flow controllers, composition analysis by gas chromatograph, and

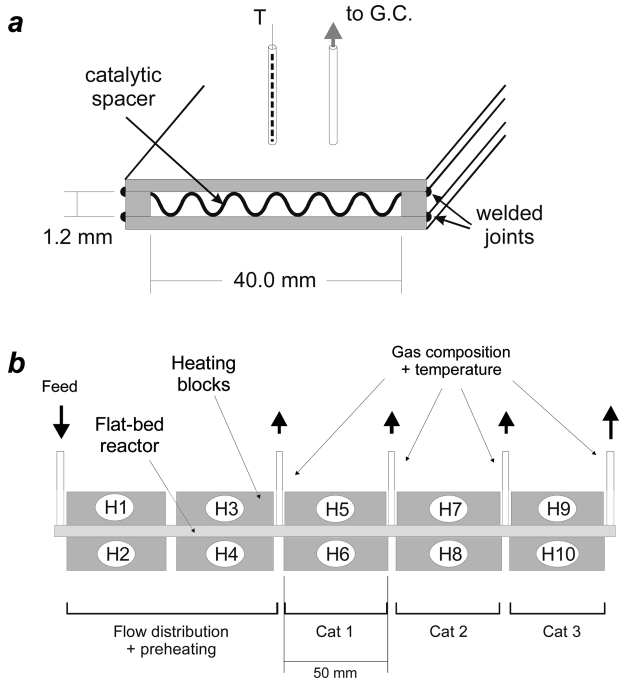

Figure 2. Schematic representation of the kinetic flat-bed reactor: (a) cross-section with corrugated catalytic spacer and conduits for composition and temperature measurement, (b) flat-bed reactor with heating blocks and side withdrawals.

automatic control and data acquisition facilities. Springmann et al.[25] reported additional details of the experimental setup.

2.2. Kinetics Measurements. Using the setup described above, axial molar fraction profiles for all components were measured under isothermal conditions for different temperatures, S/C ratios, and flow rates. Measurements were replicated 2−4 times with adequate reproducibility (relative deviations between measured concentration profiles below 5%). The explored operating conditions for the kinetic experiments are shown in Table 1. After a total of around 60 h of operation,

Table 1. Experimental Conditions for Measuring the Isothermal Kinetics of the Pd-Based Catalytic Spacers for Ethanol Steam Reforming

temperature	480−770 °C
pressure	∼ 1.2−1.5 bar
inlet concentration	1.8 < S/C < 4.7
flow rate	1.4−2.8 slpm (τ_{STP} ∼ 0.32−0.16 s)

a slight deactivation due to coking was observed for the last experiments. A few experiments at temperatures below 500 °C showed increasing amounts of higher molecular side-products (ethane, ethylene, and acetaldehyde), whereas only traces of these species were found above 580 °C.

Figure 3 reports measured axial concentration profiles as well as calculated equilibrium concentrations for reactants (Figure 3, left) and products (Figure 3, right) for operating conditions as intended for the ethanol reforming reactor. While total ethanol conversion has been achieved after the first catalytic spacer, water molar fraction continues decreasing in the second catalyst section due to methane steam reforming and water-gas shift. Equilibrium values are reached at the reactor exit. Overall, ethanol reforming can be represented at the present operating conditions by an irreversible[26] reaction of ethanol with water to

dx.doi.org/10.1021/ie202364y | Ind. Eng. Chem. Res. 2012, 51, 4143−4151

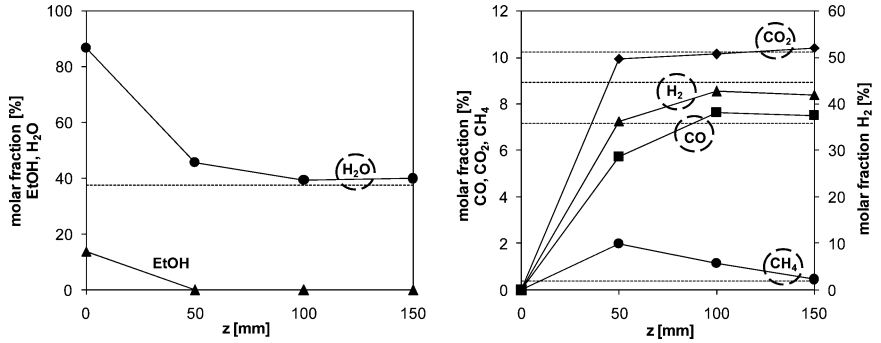

Figure 3. Molar fraction axial profiles for reactants (left) and products (right) in the kinetic flat-bed reactor. T = 690 °C, P = 1.43 bar, S/C = 3, W^+ = 176 g/h, y^+_{N2} = 0. Equilibrium values are shown as dashed lines.

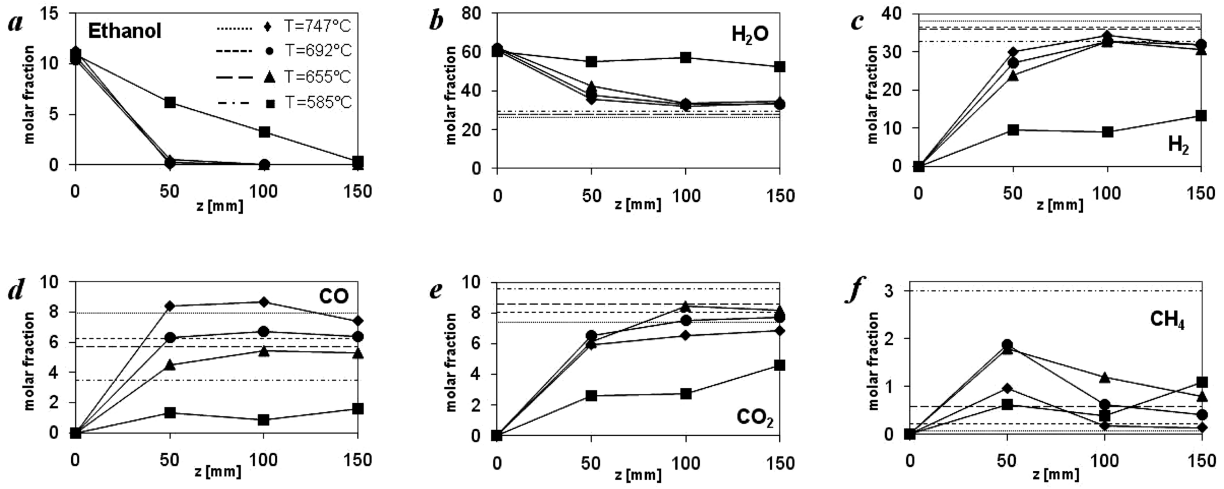

Figure 4. (a–f) Influence of operation temperature on reaction in the kinetic reactor. $P \approx$ 1.35 bar, S/C = 3, W^+ = 176 g/h, $y^+_{N2} \approx$ 0.3. Equilibrium values are shown as dotted/dashed lines.

produce carbon dioxide, methane and hydrogen (eq 1), followed by the subsequent equilibrium-limited steam reforming of methane to H_2 and CO (eq 2) and the water-gas shift reaction (eq 3).[2,26,27] This reaction scheme explains the fast depletion of ethanol and the initial increase and subsequent decrease of the methane, as shown in Figure 3.

$$C_2H_5OH + H_2O \rightarrow CH_4 + CO_2 + 2H_2 \quad (1)$$

$$CH_4 + H_2O \leftrightarrow CO + 3H_2 \quad (2)$$

$$CO + H_2O \leftrightarrow CO_2 + H_2 \quad (3)$$

The influence of temperature on species conversion is reported in Figures 4a–f. As can be seen, a temperature of around 585 °C is not sufficient at the residence time given (GHSV ≈ 23 000 1/h), to achieve complete ethanol conversion and methane is still increasing at the reactor end. At T = 655 °C ethanol is already consumed at z = 50 mm, while equilibrium values are almost reached at the reactor exit. With increasing temperature, the main reaction front moves toward the reactor entrance (Figure 4 a–d). Carbon dioxide profiles (see Figure 4e) show a nonmonotonous behavior over temperature, with a CO_2 molar fraction increase at low temperatures due to kinetic reasons and a decrease at high temperatures due to equilibrium limitations. The drop of the methane outlet concentration after an initial increase at temperatures above 585 °C is due to the increasing equilibrium conversion of the endothermic methane steam reforming reaction 2 with temperature.

Overstoichiometric S/C ratios from 2 to 4 were tested because of the following considerations: (a) the equilibrium-limited reactions 2 and 3 are promoted by an excess of water;[26] (b) an excess of water prevents the formation of coke with subsequent catalyst deactivation;[28] (c) a low concentrated ethanol/water mixture from fermentation could be used as reformer feed without extensive additional distillation.[29] Experiments with increasing S/C ratios from 2 to 4 at constant temperature and inlet flow rate result in faster reforming and higher equilibrium conversion. Since water evaporation requires additional energy, an S/C ratio of around 3 seems to represent a reasonable compromise.

2.3. Reaction Model. For modeling the kinetic experiments, a steady-state, 1-D, isothermal, pseudohomogeneous model of the flat-bed reactor was assumed. Since Bodenstein numbers were in the order of 1000–1100 for typical operating conditions, axial mass dispersion could be neglected.[30] The software PREDICI was used to simulate the reactor and to perform the nonlinear regression of the kinetic rate parameters.

The following simple mass action kinetics proved sufficient to simulate the reactor behavior in the experimentally determined range of appropriate operating conditions:

$$r_1 = k_1 p_{EtOH} p_{H_2O} \quad (4)$$

dx.doi.org/10.1021/ie202364y | Ind. Eng. Chem. Res. 2012, 51, 4143–4151

$$r_2 = k_2 p_{CH_4} p_{H_2O}\left(1 - \frac{1}{K_{eq2}}\frac{p_{CO} p_{H_2}^3}{p_{CH_4} p_{H_2O}}\right) \quad (5)$$

$$r_3 = k_3 p_{CO} p_{H_2O}\left(1 - \frac{1}{K_{eq3}}\frac{p_{CO_2} p_{H_2}}{p_{CO} p_{H_2O}}\right) \quad (6)$$

$$k_i = k_{\infty,i} e^{-E_i/RT} \quad (7)$$

The equilibrium constants appearing in eqs 5 and 6 were calculated by standard thermodynamic relations for real gases.[31]

The fitted activation energies and pre-exponential factors (see eq 7) are reported in Table 2. The obtained global activation energies are in the range reported by Graschinsky[32] and references therein. Figure 5 shows a parity plot, comparing the measured and calculated molar fractions at all withdrawal positions and for all experiments above 600 °C. For temperatures below 550 °C additional side products (acetaldehyde, ethane, ethylene) are formed and the catalyst deactivates rapidly due to coking. Therefore, no attempt was made to model the kinetics in the lower temperature range.

Table 2. Fitted Reaction Rate Parameters for the Rate Eqs 4 to 7

i	$k_{\infty,i}$ [kmol/m^3_R/seg/bar^n]	E_i [J/mol]
1	2.4×10^9	148 000
2	2.1×10^6	107 300
3	7.7×10^2	59 900

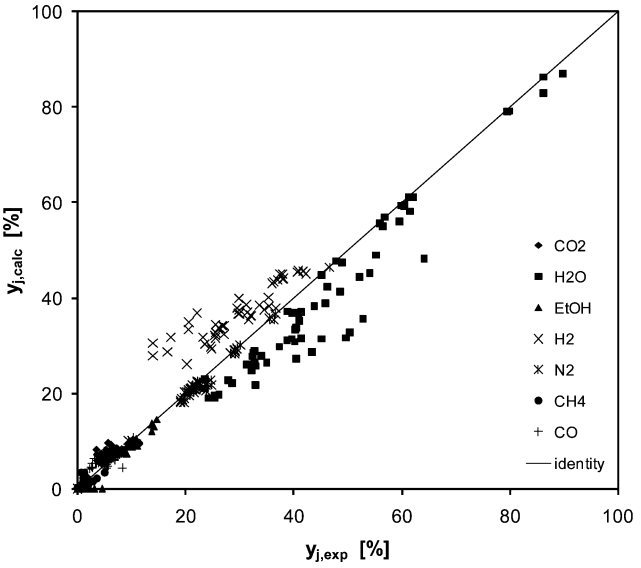

Figure 5. Parity plot for calculated vs experimental molar fractions using the fitted parameters in Table 2. 336 data points, 2.0 < S/C < 4.5, 635 < T < 750 °C, 115 < W^+ < 185 g/h, 0 < y^+_{N2} < 0.3.

3. SANDWICH REACTOR FOR THE THERMAL COUPLING OF ETHANOL STEAM REFORMING AND HYDROGEN COMBUSTION

To experimentally verify the heat integrated coupling of ethanol steam reforming and off-gas combustion, a so-called "sandwich reactor" (SR) has been set up. As shown in Figure 6, it consists of two reforming channels which sandwich a combustion channel from both sides. Since the height of each reforming channel is only half of its anticipated value, the SR is considered to represent one 2-channel module of a folded-plate reactor (FPR). The scale-up of the SR to a FPR is straightforward as demonstrated by Gritsch et al.[6] for the coupling of methane steam reforming and methane/hydrogen combustion.

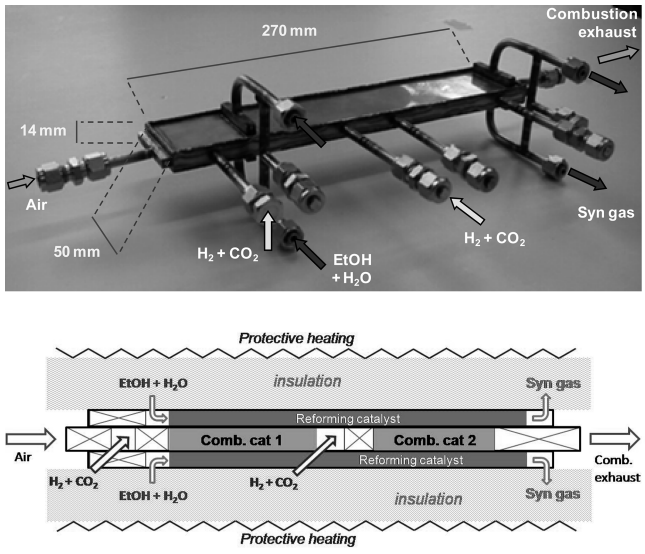

Figure 6. Photo and schematic of the 3-channel sandwich reactor for ethanol reforming.

Reforming and combustion channels are axially structured as shown in Figure 6. The catalytically coated spacers already reported in Section 2.1 were used in both channel types. One 180 mm long corrugated spacer was placed in each of the two external channels, while four 50 mm-length spacers were used in the two zones in the central combustion channel (2 spacers in each zone). Flow distributors were placed at the entrance and exit of each channel as well as after the lateral injection point for H_2 and CO_2. Stainless steel 1.4835 was employed for flow distributors and the reactor casing. The photo in Figure 6 contains the main dimensions of the sandwich reactor.

As shown in Figure 6, the combustion channel was equipped with one side-feed port. This allows splitting the fuel (hydrogen) for the combustion reaction between the reactor entrance and the side feed in order to modify the axial temperature profile. Compared to a single feed at the channel entrance, the hot spot can be reduced while adding more fuel (necessary for the operation at higher reactor loads). Also, the reactor outlet temperature of the reforming channel can thus be raised which is necessary for sufficient conversion in the reforming channels and for efficient heat recovery in case the effluent is used to preheat the reactor feed.[9] On the basis of previous experience,[23] a mixture of hydrogen with CO_2 (about 1:2 in molar ratio) is used as fuel in order to reduce the danger of homogeneous combustion of the fuel in the mixing zones. Such a mixture is typical for anode off-gas of PEM fuel cells. Experience showed that hydrogen inlet molar fractions lower than ca. 0.09 (after mixing with air) were necessary to prevent ignition of the homogeneous reaction.

Thermocouples were positioned in the inlet and outlet of each channel of the reactor and at the external-top wall of the casing to measure an axial temperature profile of the reforming channel. A moveable thermocouple was also positioned along

dx.doi.org/10.1021/ie202364y | Ind. Eng. Chem. Res. 2012, 51, 4143–4151

the external side wall of the combustion channel to obtain qualitative information of the temperature profile inside the combustion channel.

The sandwich reactor body was insulated from the environment. As indicated in Figure 6, bottom, an electric protective heating (heating temperature T_H, ca. 600 °C) was placed on both sides of the insulation to minimize heat losses. The same periphery already applied for the catalyst activity tests (see Section 2.1) was also used for the sandwich reactor. Inlet pressure of both combustion and reforming chambers was measured using pressure gauges. Molar compositions of the outlet streams were measured by gas chromatography. Additional manufacturing and implementation details can be found elsewhere.[23,25]

4. TEST RESULTS OF THE SANDWICH REACTOR

The operating conditions of the three-channel ethanol reformer are given in Table 3. Different ethanol loads were applied to

Table 3. Experimental Conditions for Ethanol Reforming in the Sandwich Reactor

T_{ref}	550−670 °C
P_{ref}	1.1−1.6 bar
S/C	2−4
V^{+}_{ref}	1.6−8.5 slpm ($\tau \approx 1.01-0.19$ s)
V^{+}_{comb}	6.8−17.7 slpm ($\tau \approx 0.29-0.11$ s)
$y_{H2}{}^{+}$	0.042−0.083
T_H	600 °C

determine the maximal capacity of the reactor. As already mentioned, an S/C ratio of 3 appeared most appropriate. Nevertheless, a variation of the S/C ratio was performed to analyze its impact on reactor performance. As already mentioned, a mixture of 33.33 mol % of hydrogen and 66.67 mol % of CO_2, has been used as burner gas to reduce the risk of homogeneous preignition of the fuel in the mixing sections. Elevated reforming temperatures (above 550 °C) were selected to ensure (nearly) complete alcohol conversion and high methane conversion. A certain drawback of elevated reforming temperatures is an increase of the CO product concentration. PEM fuel cells require a feed of purified hydrogen with only few ppm of CO in order to avoid poisoning of the Pt/Ru-based anode catalyst. Water-gas shift followed by preferential oxidation of CO (CO-PrOx) are the methods of choice for a subsequent hydrogen purification step before the fuel cell.

In addition, energy recovery from the hot reactor effluent to the entering feed should be provided in the final design. Two folded plate heat exchangers, one for the reforming and one for the combustion mixture, could be used. Such a setup already proved to be successful in the methane reformer of Gritsch,[23] requiring only a temperature difference of 50 K to transfer most of the heat of the effluent to the respective feed. To characterize the reactor performance with respect to heat recovery, the temperature differences of both combustion and reforming gas between reactor feed and exit have been recorded and will be given as ΔT_{comb} and ΔT_{ref}.

Figure 7 shows temperatures measured along the reforming channel for typical operating conditions using only front hydrogen injection in the combustion channel. Table 4 reports the composition of the stream leaving the reforming channels together with the corresponding equilibrium values and characteristic parameters which quantify the reforming and the thermal performance of the reactor. Since all hydrogen fuel

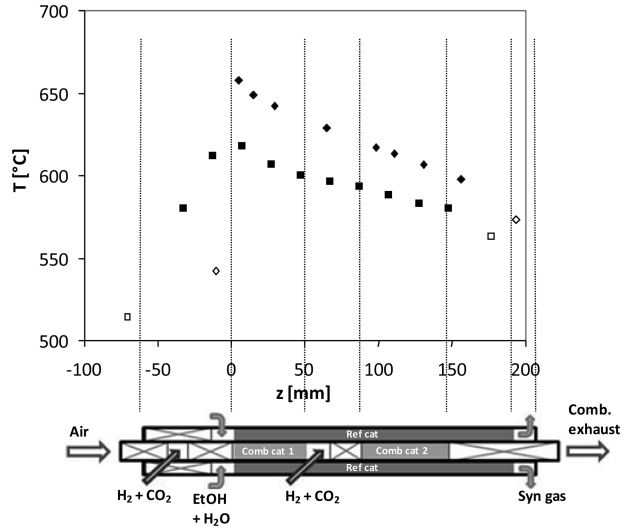

Figure 7. Measured reforming temperature profile (◆) and qualitative indication (see text) of combustion temperature profile (■). Inlet and outlet temperatures to/from each channel are specified by open symbols. W^{+}_{ref} = 402 g/h, S/C = 3, V^{+}_{comb} = 17.2 slpm (y^{+}_{H2} = 8.2%, y^{+}_{H2}/y^{+}_{CO2} = 0.5), no side injection of hydrogen, P_{ref} = 1.35 bar.

is fed to the entrance of the combustion channel, a hot spot develops at the reactor entrance, after which the reforming temperature monotonously decreases. As it was not possible to measure the temperature inside the combustion channel, only an indirect measure has been obtained by thermocouples placed at the side walls of the combustion channel. Due to lateral heat losses these temperatures are substantially lower (about 100 to 150 °C) than the true combustion channel temperatures. They are included in Figure 7 as additional information. Since feed and exit temperature for both gas streams could be measured with sufficient accuracy, the increase in sensible heat between feed and exit can be calculated. As reported below, ΔT_{comb} and ΔT_{ref} can be improved if the hydrogen fuel is split between the reactor entrance and the side-feed port.

The reforming outlet stream almost reaches equilibrium composition (see Table 4). An ethanol conversion (x_{EtOH}) of ca. 94% was measured, along with a specific hydrogen generation rate (θ^{L}_{H2}) of 50.7 slpm of hydrogen per liter of reactor and a hydrogen yield (Φ^{H2}_{EtOH}) of 4.12 mol of hydrogen per mol ethanol in feed. A parameter used in literature[23,33] to quantify the reformer performance is the "reforming efficiency" (η_{ref}, see eq 8), representing the ratio of the lower heating value LHV of hydrogen and carbon monoxide produced (CO could hypothetically be converted to H_2 by the water-gas shift reaction) and the heating value of the raw materials fed to the reactor. Unlike the hydrogen yield calculation (hydrogen produced per ethanol in feed), for the reforming efficiency calculation, fuels to both combustion and reforming chambers are considered.

$$\eta_{ref} = \frac{F^{L}_{H_2,ref}\cdot LHV_{H_2} + F^{L}_{CO,ref}\cdot LHV_{CO}}{F^{+}_{EtOH,ref}\cdot LHV_{EtOH} + F^{tot}_{H_2,comb}\cdot LHV_{H_2}} \quad (8)$$

The obtained value of η_{ref} = 0.70 indicates a good conversion efficiency for this kind of wall reactors. The remaining 30% of the heat of the reactants is divided among nonreacted ethanol, unconverted methane, increase of sensible heat (both

dx.doi.org/10.1021/ie202364y | Ind. Eng. Chem. Res. 2012, 51, 4143−4151

Table 4. Outlet and Equilibrium Compositions and Characteristic Performance Parameters for the Operating Conditions Stated in Figure 7

	molar fraction					
	H_2O	EtOH	CO	CO_2	H_2	CH_4
equilibrium	0.396	0.000	0.045	0.117	0.412	0.030
outlet	0.405	0.006	0.042	0.116	0.404	0.027
			characteristic parameters			
η_{ref}	x_{EtOH}	x_{H2}	θ^L_{H2} [$slpm_{H2}/l_R$]	$\Phi^{H2}{}_{EtOH}$	ΔT_{ref} [K]	ΔT_{comb} [K]
0.70	0.94	1	50.7	4.12	32	49

reforming and combustion streams) and losses to the environment.

4.1. Effect of Combustion Fuel Distribution. As mentioned in the Introduction, one of the great advantages of the folded-plate reactor concept over conventionally structured reactors is the easy implementation of side feeds, both with respect to their number and axial position. The exploitation of this feature for ethanol steam reforming will be analyzed in the following. Figure 8 presents a comparison between reforming temperature profiles when operating with only frontal hydrogen injection and with one additional side feed. Feeds for the combustion and reforming side are kept constant. With only frontal combustion feed, the axial temperature profile drops monotonically, whereas a more uniform profile with a second temperature maximum develops if an additional hydrogen side feed is introduced in the middle of the reactor. Both profiles have approximately the same mean temperature but the profile with distributed hydrogen injection leads to higher outlet temperatures, which is desirable for proper operation of the feed/effluent heat exchangers in the final design. No significant differences are observed in reforming efficiency. The reduced first maximum temperature due to distributed H_2 injection leads to slightly lower ethanol conversion but to higher methane conversions due to a higher outlet temperature.

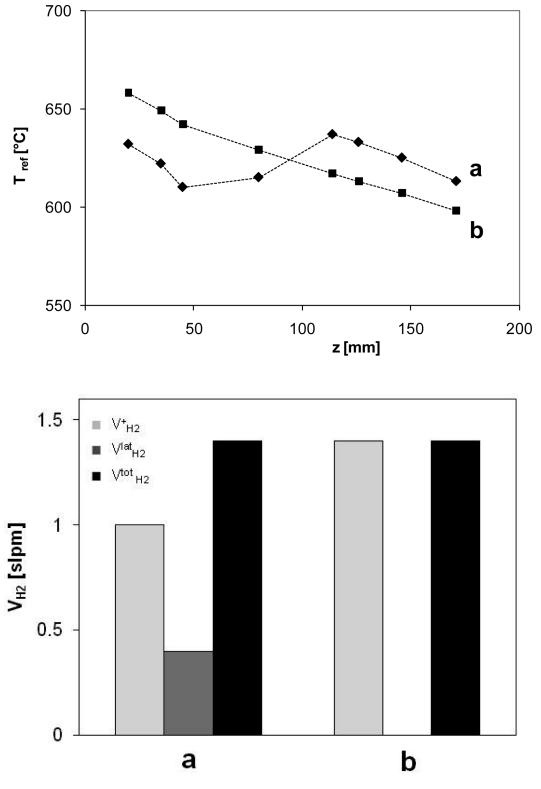

Figure 8. Reforming temperatures with (◆, a) and without (■, b) splitting the total amount of hydrogen for combustion by using the lateral injection port. W^+_{ref} = 402 g/h, S/C = 3, y^+_{H2} = 8.2% (y^+_{H2}/y^+_{CO2} = 0.5), P_{ref} = 1.34 bar.

4.2. Effect of Load Changes. Experimental results showed that the ethanol load could be doubled if the amount of burner hydrogen was adjusted. Approximately the same shape and level of the axial reforming temperature profile was achieved for

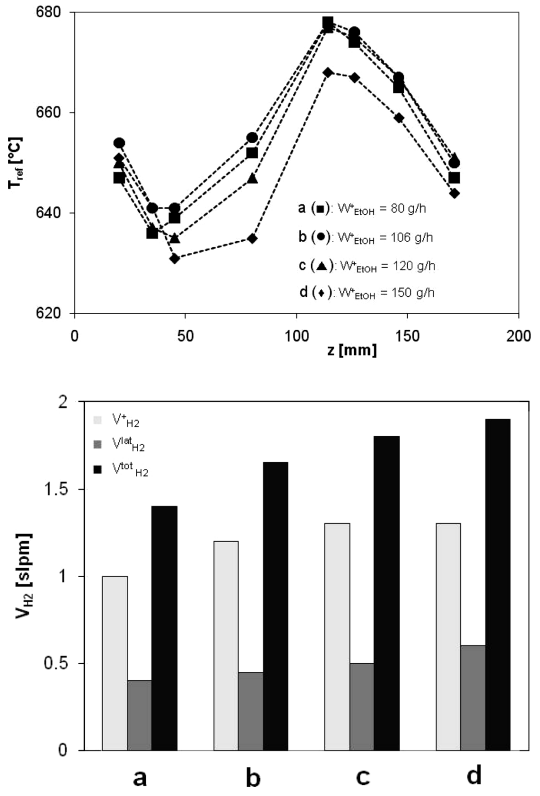

Figure 9. Reforming temperatures for different ethanol loads and total amounts of combusted hydrogen. S/C = 2, V^+_{comb} = 13.5−17.7 slpm (V^+_{H2}/V^{lat}_{H2} = 2.5, y^+_{H2} = 8.2%, y^+_{H2}/y^+_{CO2} = 0.5), P_{ref} = 1.15−1.34 bar.

Table 5. Characteristic Parameters for the Series of Experiments with Varying Ethanol Loads[a]

W^+_{EtOH} [g/h]	x_{EtOH}	η_{ref}	$\Phi^{H2}{}_{EtOH}$	θ^L_{H2} [$slpm_{H2}/l_R$]	ΔT_{ref} [K]	ΔT_{comb} [K]
80	0.950	0.72	4.27	35	57	99
106	0.955	0.74	4.27	46	68	106
120	0.956	0.73	4.19	51	75	106
150	0.944	0.73	4.01	62	74	102

[a]Operating conditions as reported in caption of Figure 9.

dx.doi.org/10.1021/ie202364y | Ind. Eng. Chem. Res. 2012, 51, 4143−4151

Table 6. Characteristic Parameters for the Series of Experiments with Varying the S/C Inlet Ratio[a]

S/C	x_{EtOH}	θ^{L}_{H2} [slpm$_{H2}$/l$_R$]	η_{ref}	Φ^{H2}_{EtOH}	ΔT_{ref} [K]	ΔT_{comb} [K]	y^{L}_{CO}	y^{L}_{CH4}
3	0.922	65	0.725	4.24	73	85	5.0	1.9
2	0.944	62	0.728	4.01	74	102	8.6	2.8

[a] W^{+}_{EtOH} = 150 g/h, V^{+}_{comb} = 15.9 slpm (y^{+}_{H2} = 8.2%, y^{+}_{H2}/y^{+}_{CO2} = 0.5), V^{lat}_{comb} = 1.8 slpm ($y^{lat}_{H2}/y^{lat}_{CO2}$ = 0.5), P_{ref} = 1.34 bar (S/C = 2), P_{ref} = 1.46 bar (S/C = 3).

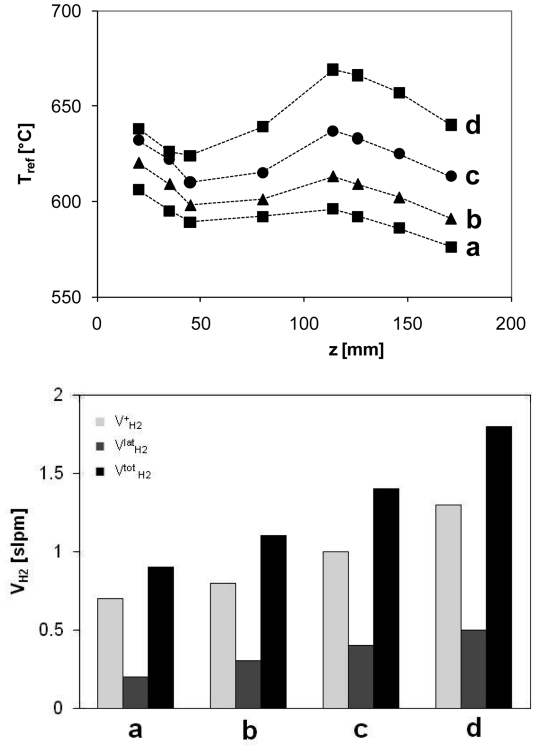

Figure 10. Axial reforming temperature profiles for different total amounts of combusted hydrogen (a–d). W^{+}_{ref} = 402 g/h, S/C = 3, V^{+}_{comb} = 9.0–17.4 slpm (y^{+}_{H2} = 8.2%, y^{+}_{H2}/y^{+}_{CO2} = 0.5), P_{ref} = 1.34 bar.

different reactor loads (Figure 9). In these experiments, the ratio between the hydrogen injected in the reactor front and in the lateral port was maintained at 2.5:1; higher flows are required at the reactor inlet in order to sufficiently preheat the ethanol/water and air feeds.

Figure 9 (bottom) shows that the required burner hydrogen needs to be increased less than proportional to maintain constant ethanol conversion of about 95% (Table 5), if the ethanol load is increased from 80 to 150 g/h. This is due to the fact that the heat losses are almost independent of the load. Table 5 reports the performance parameters for this series of experiments. The observed constancy of ethanol conversion, reforming efficiency and yield for increasing loads points at a robust operating behavior of the reactor. In all cases sufficient outlet/inlet temperature differences for both reforming (ΔT_{ref}) and combustion streams (ΔT_{comb}) have been achieved. For maximum ethanol load (150 g/h), the hydrogen production rate of the sandwich reactor amounts to a thermal equivalent of ca. 0.9 kW$_{th}$ or to a volumetric productivity of 11.3 kW$_{th}$/(liter reactor).

4.3. Effect of Changes in *S/C*. Table 6 shows the performance of the reactor if the ethanol/water inlet ratio is changed. Ethanol and combustion-H_2 loads remain unaltered

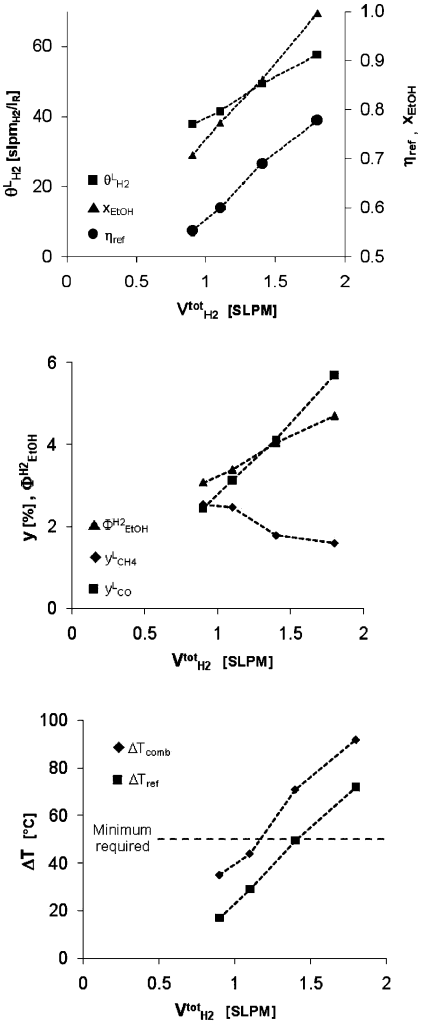

Figure 11. Characteristic parameters for the experiments with increasing combustion feed, reported in Figure 10 (operating conditions as in the caption of Figure 10).

for both experiments. The axial temperature profile measured on the reforming chamber increases by about 7 K for S/C = 2 as compared to the standard case as a result of the lower overall heat capacities in the reforming stream; for an S/C shift from 3 to 4, the temperature decreases by about 18 K. With S/C = 2, the lower water content leads to higher CO and methane product concentrations due to reduced water-gas shift and methane reforming, but also to a slight increase of ethanol conversion due to the higher temperatures. The feed/exit temperature differences for reforming and burner gas are in all cases sufficient for an efficient feed/effluent heat exchange.

Summarizing, an S/C ratio of 3 seems to be a better choice than S/C = 2 due to the higher hydrogen yield Φ^{H2}_{EtOH} and the reduced risk of catalyst coking, although the evaporation of the additional water is a cost factor in the overall energy balance.

dx.doi.org/10.1021/ie202364y | Ind. Eng. Chem. Res. 2012, 51, 4143–4151

4.4. Effect of Mean Reforming Temperature. The mean reforming temperature in the reactor can be varied by adjusting the hydrogen flow to the combustion side. Figure 10 shows the measured axial temperature profiles of the reforming chamber for a constant reformate inlet flow and different amounts of burner hydrogen which is again distributed between feed and side port at a constant ratio of 2.5 to 1. The air stream has been adjusted in each case to maintain a hydrogen molar fraction at the reactor inlet of ca. 8.2%, which represents about the maximum hydrogen concentration in air up to which homogeneous hydrogen combustion in the mixing section could be avoided.

The measured performance parameters for this series of experiments are presented in Figure 11. With higher temperatures, specific production rates of hydrogen, hydrogen yields, and ethanol as well as methane conversions increase and higher reforming efficiencies are achieved. The increases in hydrogen yield and reforming efficiency with temperature are due to the increase in both ethanol and methane conversions, despite the adverse effect for the water gas shift reaction. The required outlet−inlet temperature differences for feed/effluent heat exchange of $\Delta T > 50$ K are reached for combustion flows of H_2 higher than 1.4 slpm.

5. CONCLUSIONS

The close thermal coupling of ethanol steam reforming with hydrogen combustion on Pd-based catalysts has been studied for the production of a hydrogen-rich gas for fuel cell feeding. The catalyst was supported on a metallic corrugated spacer structure inside the reaction channels. Reaction kinetics was determined in an isothermal integral kinetic reactor, with the possibility to measure axial concentration profiles through side withdrawal ports. Above 550−600 °C, the Pd catalyst showed an adequate performance with complete ethanol conversion (no acetaldehyde), low methane outlet concentrations, and hydrogen selectivity of ca. 67% on dry basis. For subsequent mathematical modeling, a set of global reaction rate equations was fitted against experimental data. It considers ethanol decomposition (methane formation) with subsequent methane steam reforming and water-gas shift reaction. A satisfactory match between experiments and calculated data was achieved.

The thermal coupling between the endothermic ethanol steam reforming and the exothermic hydrogen combustion was studied experimentally in a three channel sandwich reactor, representing one module of a parallel plate reactor. An efficient thermal coupling between reforming and combustion was obtained. Splitting the burner fuel between the reactor entrance and a side feed port in the middle of the reactor yielded a rather uniform temperature profile and allowed for a maximum hydrogen production of 0.9 kW thermal power equivalent or 11.3 kW_{TH} per liter reactor volume. This means that very compact parallel plate reformers with thermal power between about 4 and 50 kW could be assembled from the two-channel modules, preferably using the folded sheet design. Hydrogen yields of 4−4.3 mols per mole ethanol and reforming efficiencies of 0.7−0.75 have been obtained at reforming temperatures above 600 °C, yielding outlet concentrations of carbon monoxide in the range 4−6 mol %.

AUTHOR INFORMATION

Corresponding Author

*E-mail: elopez@plapiqui.edu.ar.

Present Addresses

[§]Bayer Technology Services, D-51386 Leverkusen, Germany.
[‖]BASF SE, D-67056 Ludwigshafen, Germany.

Notes

The authors declare no competing financial interest.

ACKNOWLEDGMENTS

Support of this work through Universidad Nacional del Sur (UNS) and Consejo Nacional de Investigaciones Científicas y Tecnológicas (CONICET) is gratefully acknowledged (E.L.). This research and development project was funded by the Department Ministry of the Environment Baden-Wuerttemberg within the Framework Concept "Challenge Fuel Cell" (2006-2009) and managed by the Project Management Agency Forschungszentrum Karlsruhe (PTKA).

NOMENCLATURE

E = activation energy, J/mol
k_i, $k_{i,\infty}$ = reaction rate constant, preexponential factor (eqs 4−7), $kmol_j/(m^3_R\ s\ bar^n)$
F = molar flow rate, mol/s
GHSV = gas hourly space velocity, 1/h
K_{eqi} = equilibrium constant for reaction i
LHV = lower heating value, J/mol
P = total pressure, bar
p_j = partial pressure of component j, bar
r_i = reaction rate of reaction i (see eqs 4-6), $kmol_j/(m^3_R\ s)$
R = universal gas constant, J/(mol K)
S/C = steam to carbon ratio, mol_{H2O}/mol_C
T = temperature, °C or K
T_H = temperature of compensation heating in SR, °C
V = volumetric flow rate, slpm
W = mass flow rate, g/h
x = conversion
y = molar fraction
z = axial coordinate, mm

Greek Letters

Φ^{H2}_{EtOH} = hydrogen yield, mol^L_{H2}/mol^+_{EtOH}
η_{ref} = reforming efficiency (see eq 8)
τ = residence time, s [NPT]
θ^L_{H2} = hydrogen specific production, $slpm_{H2}/l_{Reactor}$
ΔT = temperature increment in a reactor channel (outlet−inlet), K

Subscripts

b = backward reaction (see eq 6)
calc = calculated value
CH_4 = methane
CO = carbon monoxide
CO_2 = carbon dioxide
comb = combustion channel in the SR
EtOH = ethanol
exp = experimental value
f = forward reaction (see eq 6)
H_2 = hydrogen
H_2O = water
i = reaction i (see eqs 1-3)
j = component j (j: EtOH, H_2O, CH_4, CO_2, CO, H_2, N_2)
N_2 = nitrogen
ref = reforming channel in the SR

Superscripts

+ = at the reactor mouth (frontal)
L = at the reactor outlet

lat = at the lateral injection point
tot = frontal + lateral

REFERENCES

(1) Haryanto, A.; Fernando, S.; Murali, N.; Adhikari, S. Current Status of Hydrogen Production Techniques by Steam Reforming of Ethanol: A Review. *Energy Fuels* **2005**, *19* (5), 2098.

(2) Vaidya, P. D.; Rodrigues, A. E. Insight into Steam Reforming of Ethanol to Produce Hydrogen for Fuel Cells. *Chem. Eng. J.* **2006**, *117* (1), 39.

(3) Ni, M.; Leung, D. Y. C.; Leung, M. K. H. A Review on Reforming Bio-Ethanol for Hydrogen Production. *Int. J. Hyd. Energy* **2007**, *32*, 3238.

(4) Polman, E. A.; Der Kinderen, J. M.; Thuis, F. M. A. Novel Compact Steam Reformer for Fuel Cells with Heat Generation by Catalytic Combustion Augmented by Induction Heating. *Catal. Today* **1999**, *47*, 347.

(5) Frauhammer, J.; Eigenberger, G.; von Hippel, L.; Arntz, D. a New Reactor Concept for Endothermic High Temperature Reactions. *Chem. Eng. Sci.* **1999**, *54* (15−16), 3661.

(6) Gritsch, A.; Kolios, G.; Eigenberger, G. Reaktorkonzepte Zur Autothermen Führung Endothermer Hochtemperaturreaktionen. *Chem. Ing. Tech.* **2004a**, *76*, 722.

(7) Gritsch, A.; Glöckler, B.; Lopez, E.; Morillo, A.; Eigenberger, G. Integrated Concepts for the Decentralized Production of Clean Hydrogen. *Proceedings of the 18th International Symposium on Chemical Reaction Engineering*, Chicago, USA, **2004b**.

(8) Morillo, A.; Merten, C.; Eigenberger, G.; Hermann, I.; Lemken, D. Kompaktes Faltreaktorkonzept Zur Autothermen Dampfreformierung Mit Integrierter Verdampfung und Shift-Stufe. *Chem. Ing. Tech.* **2003**, *75*, 68.

(9) Gritsch, A.; Kolios, G.; Nieken, U.; Eigenberger, G. Kompaktreformer für die Dezentrale Wasserstoffbereitstellung aus Erdgas. *Chem. Ing. Tech.* **2007b**, *79* (6), 821.

(10) Venkataraman, K.; Wanat, E. C.; Schmidt, L. D. Steam Reforming of Methane and Water-Gas Shift in Catalytic Wall Reactors. *AIChE J.* **2004**, *49* (5), 1277.

(11) Wanat, E. C.; Venkataraman, K.; Schmidt, L. D. Steam Reforming and Water−Gas Shift of Ethanol on Rh and Rh−Ce Catalysts in a Catalytic Wall Reactor. *Appl. Catal. A: Gen.* **2004**, *276* (1−2), 155.

(12) Pan, L.; Wang, S. Methanol Steam Reforming in a Compact Plate-Fin Reformer for Fuel-Cell Systems. *Int. J. Hyd. Energy* **2005**, *30* (9), 973.

(13) Casanovas, A.; Saint-Gerons, M.; Griffon, F.; Llorca, J. Autothermal Generation of Hydrogen from Ethanol in a Microreactor. *Int. J. Hyd. Energy* **2008**, *33*, 1827.

(14) Kolb, G.; Hessel, V. Micro-Structured Reactors for Gas Phase Reactions. *Chem. Eng. J.* **2004**, *98* (1−2), 1.

(15) Kiwi-Minsker, L.; Renken, A. Microstructured Reactors for Catalytic Reactions. *Catal. Today.* **2005**, *110* (1−2), 2.

(16) Friedrich, G., Gaiser, G., Eigenberger, G., Opferkuch, F., Kolios, G. *Kompakter Reaktor für katalytische Reaktionen mit integriertem Warmerucktausch. Offenlegungsschrift*. DE 197 25 378 A 1, 1998.

(17) Kolios, G.; Frauhammer, J.; Eigenberger, G. Efficient Reactor Concepts for Coupling of Endothermic and Exothermic Reactions. *Chem. Eng. Sci.* **2002**, *57*, 1505.

(18) Becker, C.; Morillo, A.; Eigenberger, G.; Hermann, I.; Lemken, D. a Novel Reactor Concept for Steam Reforming with Integrated Feed Evaporation and Water-Gas-Shift Reaction. *Chem. Ing. Tech.* **2001**, *73*, 224.

(19) Morillo, A.; Freund, A.; Merten, C. Concept and Design of a Novel Compact Reactor for Autothermal Steam Reforming with Integrated Evaporation and CO Cleanup. *Ind. Eng. Chem. Res.* **2004**, *43*, 4624.

(20) López, E.; Kolios, G.; Eigenberger, G. Structured Folded-Plate Reactor for CO Preferential Oxidation. *Ind. Eng. Chem. Res.* **2005**, *44* (25), 9659.

(21) López, E.; Kolios, G.; Eigenberger, G. Preferential Oxidation of CO in a Folded-Plate Reactor. *Chem. Eng. Sci.* **2007**, *62*, 5598.

(22) Morillo, A. *Design and Development of a Folded-Sheet Reactor Concept for Hydrogen Production by Steam Reforming of Methanol*; Ph.D. Thesis, University of Stuttgart: Stuttgart, 2007.

(23) Gritsch, A. *Wärmeintegrierte Reaktorkonzepte für Katalytische Hochtemperatur-Synthesen am Beispiel der dezentralen Dampfreformierung von Methan*; Ph.D. Thesis, University of Stuttgart: Stuttgart, 2007a.

(24) Kolios, G.; Gritsch, A.; Morillo, A.; Tuttlies, U.; Bernnat, J.; Opferkuch, F.; Eigenberger, G. Heat-Integrated Reactor Concepts for Catalytic Reforming and Automotive Exhaust Purification. *Appl. Catal. B: Environ.* **2007**, *70*, 16.

(25) Springmann, S.; Friedrich, G.; Himmen, M.; Sommer, M.; Eigenberger, G. Isothermal Kinetic Measurements for Hydrogen Production from Hydrocarbon Fuels Using a Novel Kinetic Reactor Concept. *Appl. Catal. A: Gen.* **2002**, *235*, 101.

(26) Mas, V.; Kipreos, R.; Amadeo, N.; Laborde, M. Thermodynamic Analysis of Ethanol/Water System with the Stoichiometric Method. *Int. J. Hyd. Energy* **2006**, *31*, 21.

(27) Idriss, H.; Scott, M.; Llorca, J.; Chan, S. C.; Chiu, W.; Sheng, P. Y.; Yee, A.; Blackford, M. A.; Pas, S. J.; Hill, A. J.; Alamgir, F. M.; Rettew, R.; Petersburg, C.; Senanayake, S.; Barteau, M. A. A Phenomenological Study of the Metal/Oxide Interface. The Role of Catalysis in Hydrogen Production from Renewable Sources. *ChemSusChem* **2008**, *1*, 905.

(28) Comas, J.; Mariño, F.; Laborde, M; Amadeo, N. Bio-Ethanol Steam Reforming on Ni/Al_2O_3 catalyst. *Chem. Eng. J.* **2004**, *98* (1−2), 61.

(29) Rass-Hansen, J.; Johansson, R.; Møller, M.; Christensen, C. Steam Reforming of Technical Bioethanol for Hydrogen Production. *Int. J. Hyd. Energy* **2008**, *33* (17), 4547.

(30) Hessel, V.; Renken, A.; Schouten, J; Yoshida, J. *Micro Process Engineering: A Comprehensive Handbook*; Wiley-VCH: Weinheim, Germany, 2009; Vol. *1*.

(31) Smith, J. M.; Van Ness, H. C.; Abbott, M. *Introduction to Chemical Engineering Thermodynamics*; McGraw-Hill: New York, 2004.

(32) Graschinsky, C.; Laborde, M.; Amadeo, N.; Le Valant, A.; Bion, N.; Epron, F.; Duprez, D. Ethanol Steam Reforming over Rh(1%)-$MgAl_2O_4/Al_2O_3$: A Kinetic Study. *Ind. Eng. Chem. Res.* **2010**, *49*, 12383.

(33) Giroudière, F.; Sanger, R.; His, S.; Boyer, C.; Doshi, K.; Xu, J. Production of Hydrogen from Bio-ethanol. WHEC 16, 13−16 June 2006, Lyon, France, 2006.